DOI 10.1007/s11182-015-0522-9

Russian Physics Journal, Vol. 58, No. 4, August, 2015 (Russian Original No. 4, April, 2015)

BEHAVIOR OF MACROFRAGMENTATION OF SHEAR-INDUCED DEFORMATION AND OF REORIENTATION OF MACROREGIONS FORMED IN ALUMINUM SINGLE CRYSTALS UNDER COMPRESSION

L. A. Teplyakova[1] and I. V. Bespalova[2]

UDC 669.017.539.4

Results of investigations into the behavior of plastic deformation macrofragmentation and macrolocalization in aluminum single crystals in which constrained shear volumes can be distinguished for the family of {111} planes under maximum loading are presented. Single crystals with the following three orientations: $[\bar{1}11]$, $[1\bar{1}2]$, and [001] are investigated. It is established that in such single crystals, plastic deformation macrolocalization is observed under uniaxial compression with the formation of reorientation regions whose shapes and sizes depend on the single crystal orientation.

Keywords: single crystal, deformation relief, shear-induced deformation, deformation localization.

INTRODUCTION

As a rule, localization of shear-induced deformation on different scale-structural levels occurs under compression of single crystals of metals and alloys with the FCC lattice [1–7]. The range of scales in which the localization is intensively manifested and the localization mechanism depend on many factors, including the possibilities of easy shear along the slip planes having the maximum Schmid factors. Thus, in [6, 7] it was established that in single crystals with easy shear volumes, strongly pronounced localization of the shear-induced deformation accompanied by the formation of slip macropackets was observed from the very onset of plastic deformation. Otherwise, the situation was observed in single crystals in which the possibility of shear crossing the free faces of crystals having such geometry was impeded by the circumstance that in a part of the single crystal volume, the slip planes and systems appeared *locked* (bounded by the crystal end faces) [8]. In such single crystals, considerable reverse stresses facilitating the accumulation of the excess dislocation density must arise. With further increase in deformation, smooth and discrete misorientations of local volumes can arise in such single crystal regions on various scales. The present work is devoted to a study and generalization of the behavior of misorientations arising on the macrolevel in aluminum single crystals in which constrained shear volumes can be distinguished before or during loading when the sample changes its shape. The samples were deformed by uniaxial compression at room temperature. Details of the experiment were described in [7, 8].

1. RESULTS AND DISCUSSION

In the present work, the group of single crystals was investigated whose volumes were bounded from two sides by the end faces of the sample – constrained shear volumes (CSVs). Single crystals with the following orientation of the

[1]Tomsk State University of Architecture and Building, Tomsk, Russia; [2]Kazakh National Technical University, Almaty, Kazakhstan Republic, e-mail: lat168@mail.ru; besiv@mail.ru. Translated from Izvestiya Vysshikh Uchebnykh Zavedenii, Fizika, No. 4, pp. 33–38, April, 2015. Original article submitted January 16, 2015.

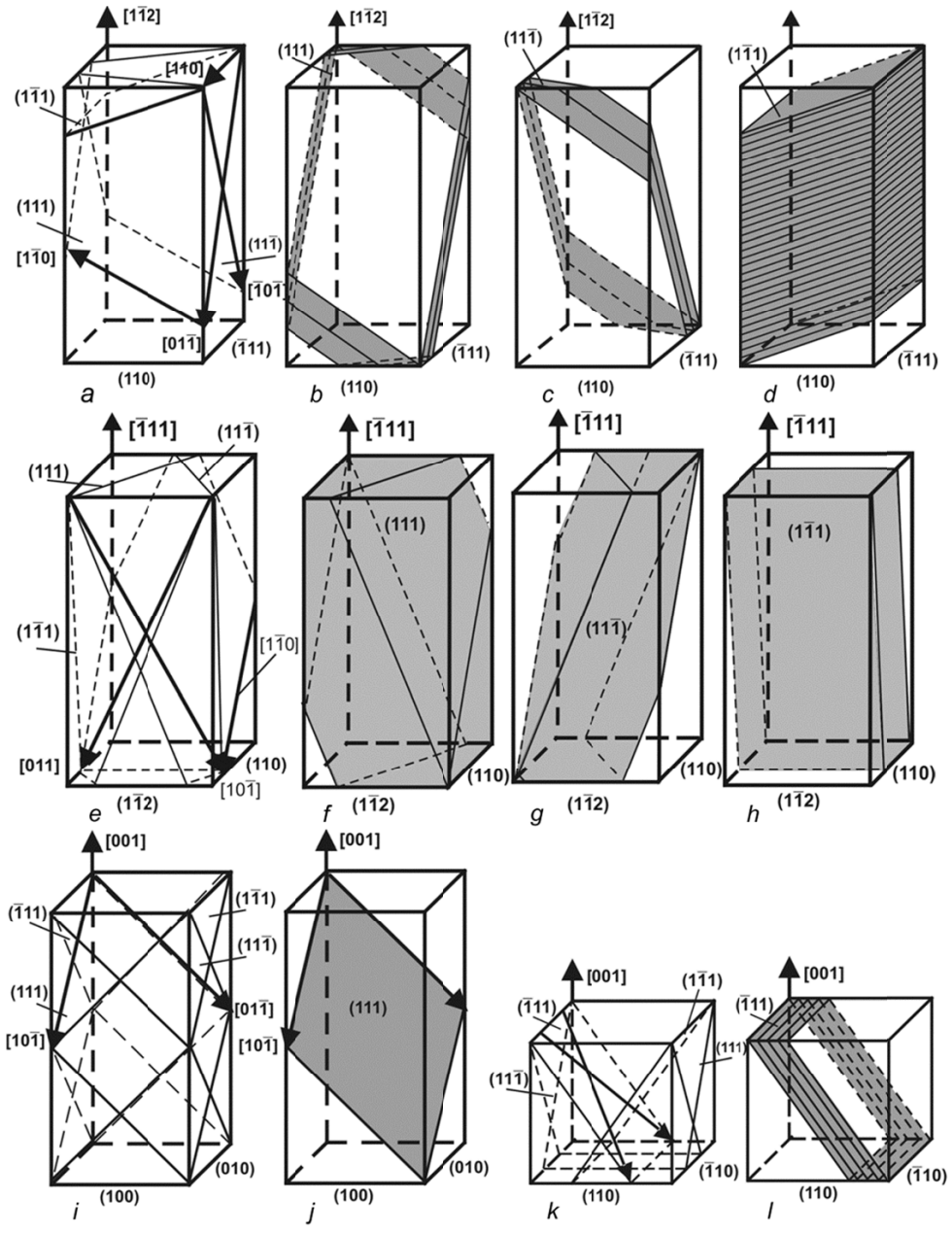

Fig. 1. Crystallographic scheme of orientation of the {111} loaded planes in the $[\bar{1}11]$, $[1\,\bar{1}2]$, and [001] single crystals (*a*, *e*, *k*, and *i*); scheme of the CSV distinguished for the families of equiloaded planes (*b*–*d*, *f*, *g*, and *l*); scheme of the distinguished ESV (*h*); and scheme of the distinguished constrained shear plane (*j*).

compression axis: 1) $[1\,\bar{1}2]$ – **FT** single crystals, 2) $[\bar{1}11]$ – **T** single crystals, and 3) [001] – **F** single crystals belong to this group (here $\mathbf{F1_k}$ are cubic single crystals with the {110} side faces and **F2** are single crystals with the {001} side faces). All samples were shaped as parallelepipeds with linear sizes 3 × 3 × 6 mm, except for the cubic crystal with sizes 3 × 3 × 3 mm. In the **FT** single crystals, two $(111)[0\,\bar{1}1]$ and $(11\,\bar{1})[101]$ octahedral sliding systems with the Schmid factor equal to 0.41 (Fig. 1*a*) were equiloaded. Volumes in which slip planes were bounded by the end faces, that is, the CSVs (Fig. 1*b* and *c*) can be distinguished for them together with the volume in which sliding planes crossed

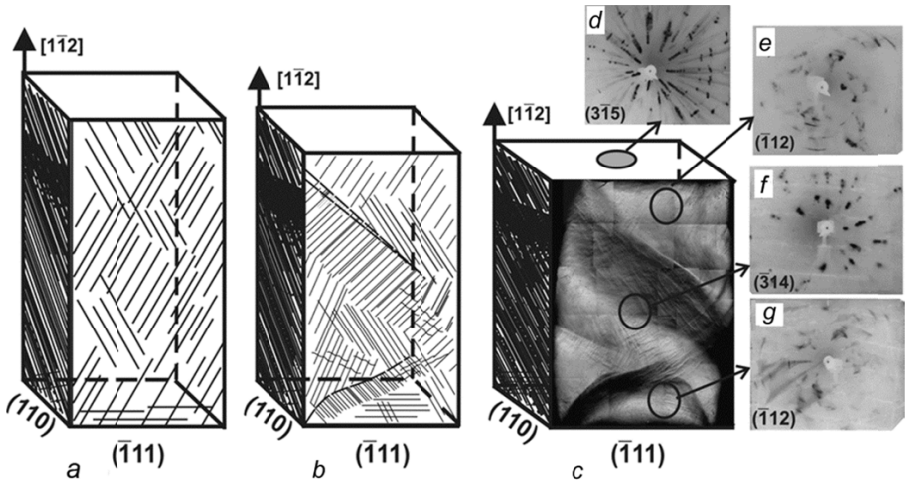

Fig. 2. Scheme of the pattern of the strain relief in single crystals at ε = 0.06 (*a*), 0.13 (*b*), and 0.20 (*c*) and the lauegrams recorded under irradiation of the single crystal (*d*–*g*).

all side faces of the single crystal, that is, the easy shear volume (ESV) (Fig. 1*d*) for the family of the $(11\bar{1})$ planes (with the Schmid factor equal to 0.27). In the **T** single crystals, octahedral slip planes were equiloaded (Fig. 1*e*). Moreover, the CSV can be distinguished for each of them in the single crystal (Fig. 1*f*–*h*). In the $\mathbf{F1_k}$ single crystals, all octahedral planes were equiloaded (Fig. 1*k*), and the CSVs can be distinguished for each of them (Fig. 1*l*). In the **F2** single crystals before loading, only the constrained shear planes could be distinguished in each of four families of the {111} equiloaded planes (Fig. 1*i* and *j*).

FT single crystals. At small strain degrees, the main elements of the deformation relief on the *macrolevel* in the FT aluminum single crystals are: 1) shear traces on the loaded octahedral planes, 2) thin deformation folds approximately parallel to the shear traces, 3) localized slip bands, and 4) regions of bend faces (Fig. 2). Further increase in the deformation of the FT single crystals leads to an increased density of localized shear bands and complication of their internal structures. At ε = 0.2, the macrofragment with the clear-cut boundary is formed in the single crystal volume; it occupied no less than one third of the crystal volume (Fig. 2*c*). The angles of deviation of the shear traces from the nearest crossing octahedral planes were measured. Based on our measurements, it was established that the above-discussed macrofragment was misoriented relative to the neighboring single crystal regions. At this strain degree (ε = 0.2), lauegrams and epigrams of the entire sample volume were recorded in three mutually perpendicular directions: perpendicularly to the end face of the sample and to its (110) and $(\bar{1}11)$ side faces. Figure 2*c* shows regions of the sample onto which the primary beam was directed and the lauegrams that were recorded. The asterism of the lauegram spots is well pronounced, which testifies to the occurrence of continuous misorientations in the deformed single crystal.

As a result of interpretation of the lauegram recorded under irradiation along the single crystal compression axis (Fig. 2*d*), indices of the $(3\bar{1}5)$ planes were obtained. The angle between the normals to the $(3\bar{1}5)$ and $(1\bar{1}2)$ planes was 14°. Measurement of the radial misorientation from blurring of spots in the examined lauegram (Fig. 2*d*) yielded the same result – 14°. The lauegram spots were blurred not only in the radial direction. In the azimuth direction, they were split into two-three spots, which testified to the occurrence of discrete misorientations in the crystal.

The lauergams of different regions of the $(\bar{1}11)$ face differed considerably from each other and had a complicated structure of the spots (Fig. 2, *e*–*g*). Interpretation of the stereographic projections demonstrated that the main contribution to the spot pattern of the lauegram near the end faces came from the $(\bar{1}12)$ planes (the angle of deviation from the $(\bar{1}11)$ face was 11°). In the region of the reorientation bands, the main contribution came from the

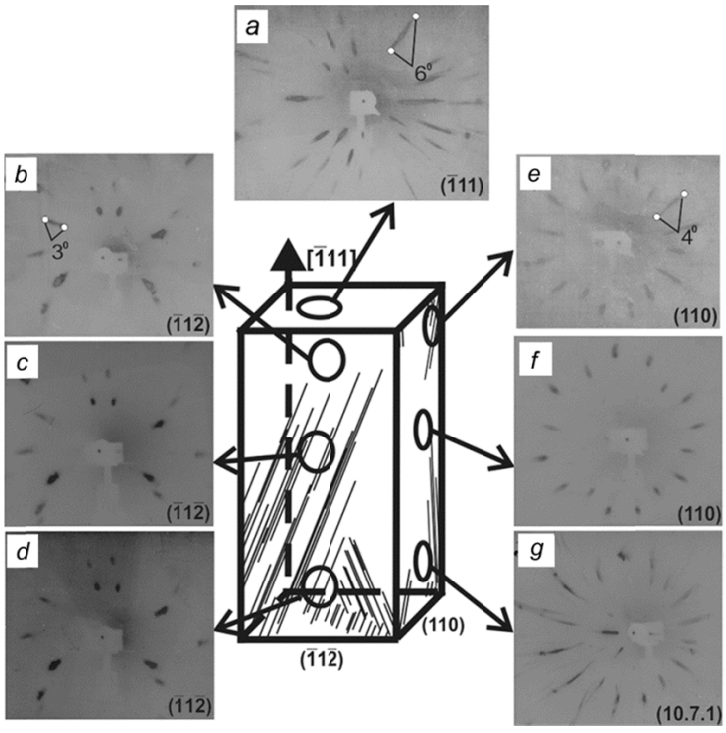

Fig. 3. Scheme of the pattern of the deformation relief for the $[\bar{1}11]$ single crystal at $\varepsilon = 0.06$ and the lauegrams recorded under irradiation of the single crystal.

$(3\bar{1}4)$ planes. The angle between the normals to this plane and to the $(\bar{1}11)$ plane was equal to 25°. The results obtained confirmed the conclusion about the formation of the crystal lattice in the $[1\bar{1}2]$ single crystal during deformation of the reorientation macroregion made above from the shear trace pattern.

***T* single crystals.** At small strain degrees, the most part (70–80%) of the face surfaces of the T single crystals was occupied by systems of small deformation folds resembling protrusions rather than by systems of long traces of the octahedral shear typical for single aluminum crystals of other orientations [4, 7] (Fig. 3). In addition, systems of deformation macrobands of various types were formed in the sample volume (Fig. 3). At $\varepsilon = 0.06$, the boundaries of the deformation bands, as a rule, deviated from the intersection of the nearest equiloaded octahedral planes at angles of 5–6°. We also recorded the lauegrams of the T single crystal regions ($\varepsilon = 0.06$). The asterism of the spots was well pronounced for all recorded lauegrams, which testified to the occurrence of continuous misorientations in the deformed single crystal. Measurement of the radial misorientation from blurring of the lauegram spots (Fig. 3*a*) yielded values ranging from 2 to 6°. Analogous result was also obtained for the lauegrams shown in Fig. 3*b–d.* Interpretation of the lauegrams shown in Fig. 3*e* and *f* yielded the indices of the planes (110). Interpretation of the lauegram recorded near the end face of the crystal (Fig. 3*g*) demonstrated that the main contribution to the spot pattern in the lauegram came from the planes (10.7.1). The angle between the normals to this plane and to the face plane was 11°.

This suggests that the presence of the CSV is the main reason for the instability on the macrolevel of the shear-induced deformation along the octahedral planes in the FT and T single crystals. As a result, macroregions (macrofragments) misoriented relative to the neighboring fragments are formed in both single crystals during deformation.

F1*$_k$ *single crystals. In these single crystals, the ESVs are distinguished for all families of the octahedral planes. It was established that the shear macrolocalization was observed in two of four equiloaded families of the {111} planes and that two shear macrobands were formed that crossed through the single crystal. They were located exactly in the ESVs for these planes. When the sample height was halved **(F1$_k$** single crystals**),** the CSV rather than the ESV were

TABLE 1. Primary Macrofragmentation and Localization of Shear-Induced Deformation in Single Crystals with the Constrained Shear Volume.

Orientation of the compression axis and side faces of single crystals	FT [1$\bar{1}$2] (110) ($\bar{1}$11)	T [$\bar{1}$11] (1$\bar{1}$2) (110)	F1$_k$ [001] F2 {110} {100}
Schmid's factor	0.40 0.27	0.27	0.40
Constrained and easy shear volumes	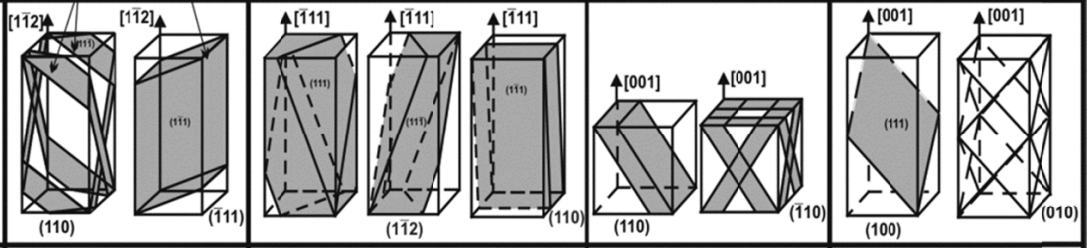		
Primary shear fragmentation	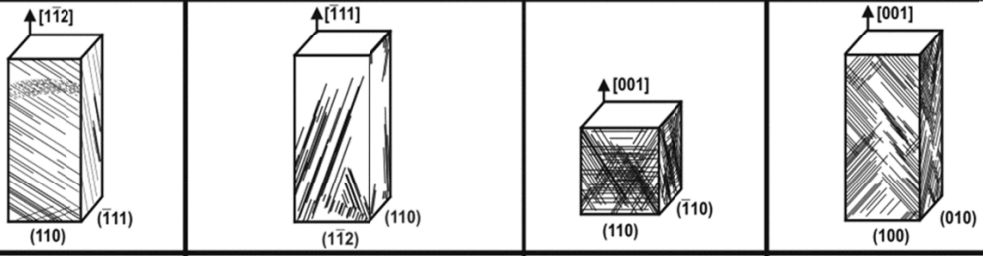		
Shear localization	Reorientation macroband	Systems of deformation macrobands	Incomplete shear macrobands / Absent

distinguished for the families of the {111} planes**.** In each of the side faces of the F1$_k$ single crystal, shear traces were observed along all octahedral planes, and in one of the two tilted systems of traces, two narrow macropackets of shear traces were observed (see Table 1). They spread from the apexes of the upper and lower end faces toward each other along the boundaries of the CSV crossing the single crystal face. Investigation of the deformation relief of *all* side faces of the single crystal demonstrated that macropackets of traces were formed due to shear along the four families of the octahedral planes, rather than along two of them as in the F1 single crystals. In addition, the macropackets of traces in the F1$_k$ single crystals were formed due to the shear along the {111} planes. They did not cross the entire single crystal, that is, they resulted from the incomplete shear. Thus, the change of the single crystal geometry from F1 to F1$_k$ and the change of the scheme of the main stresses [9] resulted in a more homogeneous plastic deformation.

F2 single crystals. First of all, we note that patters of the deformation relief formed on all free faces of the single crystal were analogous (Table 1). On each of them, as expected, two systems of shear traces parallel to the crossing lines of the two of four equiloaded octahedral planes were formed. In local face regions, one system of shear traces was observed more often than the crossed systems of traces. The majority of systems of shear traces attenuated toward the middle of the faces. All this testified to the development of the primary macrofragmentation of shear-induced deformation in the F2 single crystals. The localization of shear-induced deformation on the macrolevel was absent. It seemed likely that the absence of the easy shear volume for each of the equiloaded families of the {111} planes in the F2 single crystals predetermined the impossibility of shear-induced deformation macrolocalization due to shear along the macropackets that crossed through the single crystal as was the case for the single crystals with the same orientation of the compression axis, but with the {110} side faces (F1 single crystals) [4, 10]. The above-indicated fact demonstrates that for spatial organization of the shear and deformation localization on the macrolevel under compression not only the crystallographic orientation of the loading axis, but also the orientation of the single crystal faces is important. We note that the behavior of the shear macrofragmentation in the F2 single crystals of the Ni_3Fe alloy was in general analogous to that in the F2 aluminum single crystals [11]. However, a lower number of stacking fault defects in Ni_3Fe and, as a consequence, a stronger affinity to the shear planes promoted essential strengthening of

the shear asymmetry in the families of the octahedral planes, thereby causing the formation of larger primary shear macrofragments.

CONCLUSIONS

In this work, results of investigation into the spatial organization of shear-induced deformation in aluminum single crystals whose compression axes lie on the $[001]-[\bar{1}11]$ straight line of the standard stereographic triangle have been presented. The feature in common for these single crystals was that no easy shear volume could be distinguished in them for maximum loaded planes; on the contrary, the constrained shear volume could be distinguished (see Table 1). The F2 single crystals in which the constrained shear plane rather than the constrained shear volume was observed occupied a special place in this group; however, constrained shear volumes were formed in them during deformation, and their relative fraction increased during compression.

The behavior of plastic deformation in the single crystals of this group is reduced to the following.

1. In all examined single crystals, the *primary* shear macrofragmentation along the loaded octahedral planes developed from the very onset of plastic deformation. In the FT, $F1_k$, and F2 single crystals this was caused by the inhomogeneous incomplete (not crossing through) shear along these planes. In the T single crystals, such macrofragments occupied no more than 20% of the single crystal volume.

2. In single crystals in which the *constrained shear* volumes were distinguished for the families of equiloaded octahedral planes, deformation macrolocalization occurred during plastic deformation causing the formation of reorientation macroregions in the FT single crystals, deformation macrobands in the T single crystals, and incomplete shear macropackets in the $F1_k$ single crystals. When the height of the F1 single crystal was halved, this led to the change of the character of macrolocalization. Whereas macrolocalization in the F1 single crystals was observed in two of four families of equiloaded octahedral planes with the formation of the shear macropackets that crossed through the single crystal, macrolocalization in the F1k single crystals was observed in each of four families of equiloaded octahedral planes also with the formation of shear macropackets; however, they were attenuated in the sample volume.

3. No localization of shear deformation was observed on the macrolevel in the aluminum single crystals when the orientation of the side faces changed from F1 to F2.

REFERENCES

1. R. W. K. Honeycombe, Plastic Strain of Metals [Russian translation], Mir, Moscow (1974).
2. H. Neuhauser, Dislocat. Solids, **8**, 319–440 (1983).
3. Yu. A. Abzaev, V. A. Starenchenko, Yu. V. Solovyova, *et al*., Prikl. Mekh. Tekh. Fiz., **39**, No. 1, 154–159 (1998).
4. L. A. Teplyakova and É. V. Kozlov, Fizich. Mesomekh., **8**, No. 6, 57–66 (2005).
5. D. V. Lychagin, S. Yu. Tarasov, A. V. Chumaevskii, *et al*., Izv. Vyssh. Uchebn. Zaved. Fiz., **56**, No. 12/2, 60–65 (2013).
6. L. A. Teplyakova, T. S. Kunitsyna, V. A. Starenchenko, *et al*., Russ. Phys. J., **57**, No. 2, 206–215 (2014).
7. I. V. Bespalova and L. A. Teplyakova, Russ. Phys. J., **57**, No. 2, 230–236 (2014).
8. L. A. Teplyakova, I. V. Bespalova, and D. V. Lychagin, Fizich. Mesomekh., **12**, No. 2, 67–76 (2009).
9. S. I. Gubkin, Theory of Metal Processing by Pressure [in Russian], Metallurgizdat, Moscow (1947).
10. D. V. Lychagin, L. A. Teplyakova, R. V. Shaekhov, *et al*., Fizich. Mesomekh., **6**, No. 3, 75–83 (2003).
11. L. A. Teplyakova, I. V. Bespalov, and. T. S. Kunitsyna, Vestn. Permsk. Natsion. Issled. Univ., No. 3, 218–233 (2012).